

**Supporting information for**

**POSS Solid Solutions Exhibiting Orientationally**

**Disordered Phase Transition**

**Satoshi Morimoto, Hiroaki Imoto, and Kensuke Naka\***

**Materials**

Heptaisobutyl-hydride- $T_8$  cage (H-POSS),<sup>[1]</sup> heptaisobutyl-vinyl- $T_8$  cage (V-POSS),<sup>[2]</sup> heptaisobutyl-allyl- $T_8$  cage (A-POSS),<sup>[3]</sup> and hexaisobutyl- $T_8$  cage (iBu-POSS)<sup>[4]</sup> were prepared according to the previous reports.

Other mono-functionalized-heptaisobutyl- $T_8$ -silsesquioxanes (Me-POSS, SH-POSS) were prepared referring to the reported general corner capping reaction.<sup>[5, 6]</sup>

**Synthesis of heptaisobutyl-methyl- $T_8$  cage (Me-POSS)**

Me-POSS was prepared by corner-capping reaction of heptaisobutyl incompletely condensed POSS (5.01 g, 6.33 mmol) with trichloromethylsilane (0.89 ml, 7.58 mmol). Yield: 66%

$^1\text{H-NMR}$  ( $\text{CDCl}_3$ ,  $\delta$  in ppm):  $\delta$  1.81-1.91 (m,  $\text{CH}_2\text{CH}(\text{CH}_3)_2$ , 7H), 0.95 (d,  $J = 6.6$  Hz,  $\text{CH}_3$ , 42H), 0.59-0.61 (m,  $\text{CH}_2\text{-Si}$ , 14H), 0.12 (s,  $\text{Si-CH}_3$ , 3H).

$^{29}\text{Si-NMR}$  ( $\text{CDCl}_3$ ,  $\delta$  in ppm):  $\delta$  -66.1, -67.9 ( $T_8$  cage).

$^{13}\text{C-NMR}$  ( $\text{CDCl}_3$ ,  $\delta$  in ppm):  $\delta$  25.6 ( $\text{CH}_2\text{CH}(\text{CH}_3)_2$ ), 23.8 ( $\text{CH}_2\text{CH}(\text{CH}_3)_2$ ), 22.4

(CH<sub>2</sub>CH(CH<sub>3</sub>)<sub>2</sub>), 4.60 (Si-CH<sub>3</sub>).

### Synthesis of heptaisobutyl-mercaptopropyl-T<sub>8</sub> cage (SH-POSS)

SH-POSS was prepared by corner-capping reaction of heptaisobutyl incompletely condensed POSS (5.07 g, 6.32 mmol) with trimethoxy-3-mercaptopropylsilane (1.40 ml, 7.58 mmol)). Yield: 27%

<sup>1</sup>H-NMR (CDCl<sub>3</sub>,  $\delta$  in ppm):  $\delta$  2.51-2.57 (m, CH<sub>2</sub>CH<sub>2</sub>CH<sub>2</sub>SH, 2H), 1.79-1.92 (m, CH<sub>2</sub>CH(CH<sub>3</sub>)<sub>2</sub>, 7H), 1.67-1.75 (m, CH<sub>2</sub>CH<sub>2</sub>CH<sub>2</sub>SH, 2H), 1.29-1.33 (m, CH<sub>2</sub>CH<sub>2</sub>CH<sub>2</sub>SH, 1H), 0.95 (d, J = 6.8 Hz, -CH<sub>3</sub>, 42H), 0.71-0.75 (m, CH<sub>2</sub>CH<sub>2</sub>CH<sub>2</sub>SH, 2H), 0.59-0.62 (m, Si-CH<sub>2</sub>, 14H),.

<sup>29</sup>Si-NMR (CDCl<sub>3</sub>,  $\delta$  in ppm):  $\delta$  -67.6, -67.9 (T<sub>8</sub> cage).

<sup>13</sup>C-NMR (CDCl<sub>3</sub>,  $\delta$  in ppm):  $\delta$  41.6 (CH<sub>2</sub>CH<sub>2</sub>CH<sub>2</sub>SH), 27.5 (CH<sub>2</sub>CH<sub>2</sub>CH<sub>2</sub>SH), 25.6 (CH<sub>2</sub>CH(CH<sub>3</sub>)<sub>2</sub>), 23.8 (CH<sub>2</sub>CH(CH<sub>3</sub>)<sub>2</sub>), 22.4 (CH<sub>2</sub>CH(CH<sub>3</sub>)<sub>2</sub>), 11.2 (CH<sub>2</sub>CH<sub>2</sub>CH<sub>2</sub>SH).

### Measurements

Differential scanning calorimetry (DSC) was measured on a DSC-60 Plus, Shimadzu Thermogravimetric Analyzer (Shimadzu, Kyoto, Japan). Powder X-ray diffractometry (XRD) studies were performed on a Rigaku Smartlab X-ray diffractometer with Cu K $\alpha$  radiation ( $\lambda$  = 1.5406 Å) in the  $2\theta/\theta$  mode at room temperature. The  $2\theta$  scan data were collected at 0.01° intervals and the scan speed was 5° ( $2\theta$ ) / min. Thermal conductivity was measured on a Rigaku C-Therm TCI

Max-k. A pellet sample with a diameter of 20 mm and 3 mm thickness was prepared by pressing at 300 kg/cm<sup>2</sup> for 1 min at room temperature.

[1] (a) C.-H. Lu, C.-H. Tsai, F.-C. Chang, K.-U. Jeong, S.-W. Kuo, *J. Colloid Interface Sci.* 2011, 358, 93. (b) M. Takeda, K. Kuroiwa, M. Mitsuishi, J. Matsui, *Chem. Lett.* 2015, 44, 1560-1562. (c) H. Imoto, *Polym. J.* 47, 609-615.

[2] P. Zak, C. Pietraszuk, B. Marciniec, G. Spólnik, W. Danikiewicz, *Adv. Synth. Catal.* **2009**, 351, 2675-2682.

[3] Y. Yasumoto, *Polym. J.*, 2016, 48, 281-287.

[4] C. Jost, A. Kuehnle, H. C. L. Abbenhuis, *PCT Int. Appl.*, 2003042223, 22 May 2003

[5] I. Blanco, L. Abate, A. Bottino, P. Bottino, *J. Therm. Anal. Calorim.*, **2012**, 108, 807.

[6] W. Zhang, A. H. E. Muller, *Polymer*, **2010**, 51, 2133.

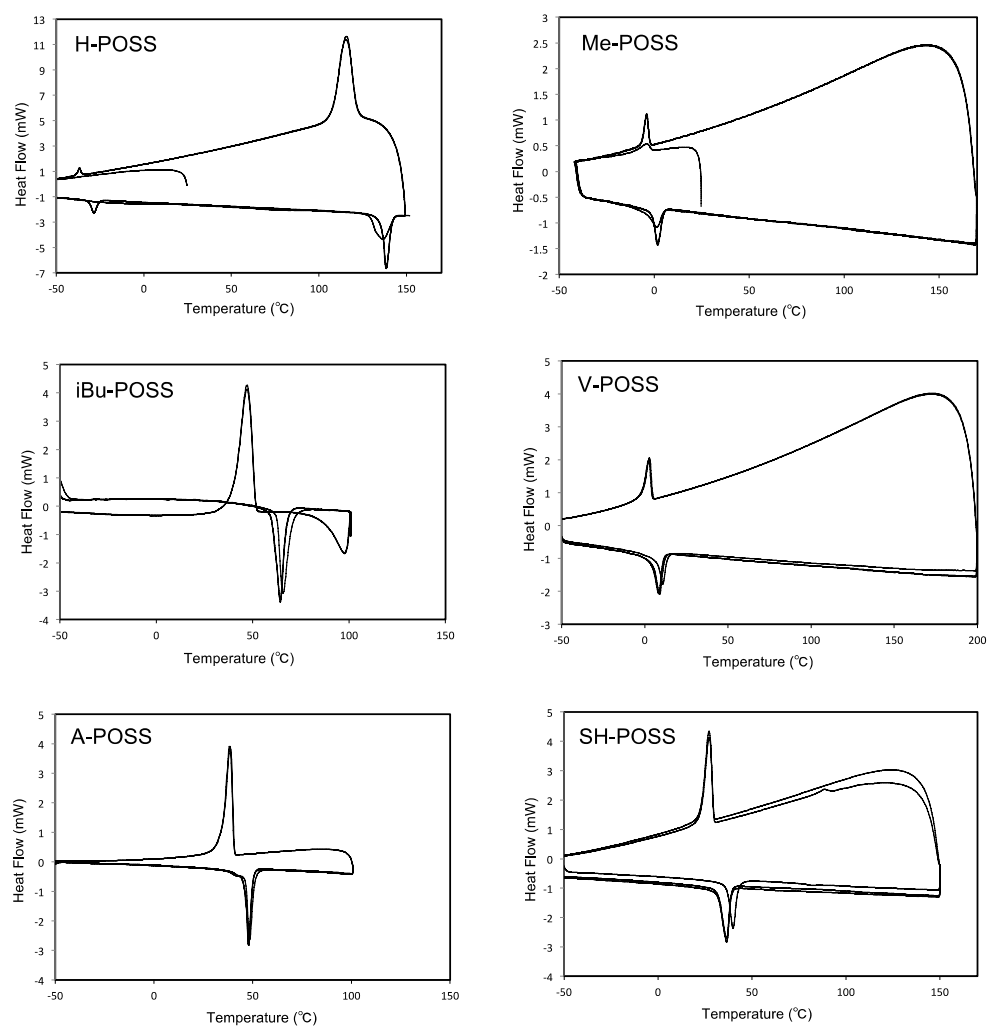


**Figure S1** DSC traces of the mono-functionalized POSS (R-POSS).

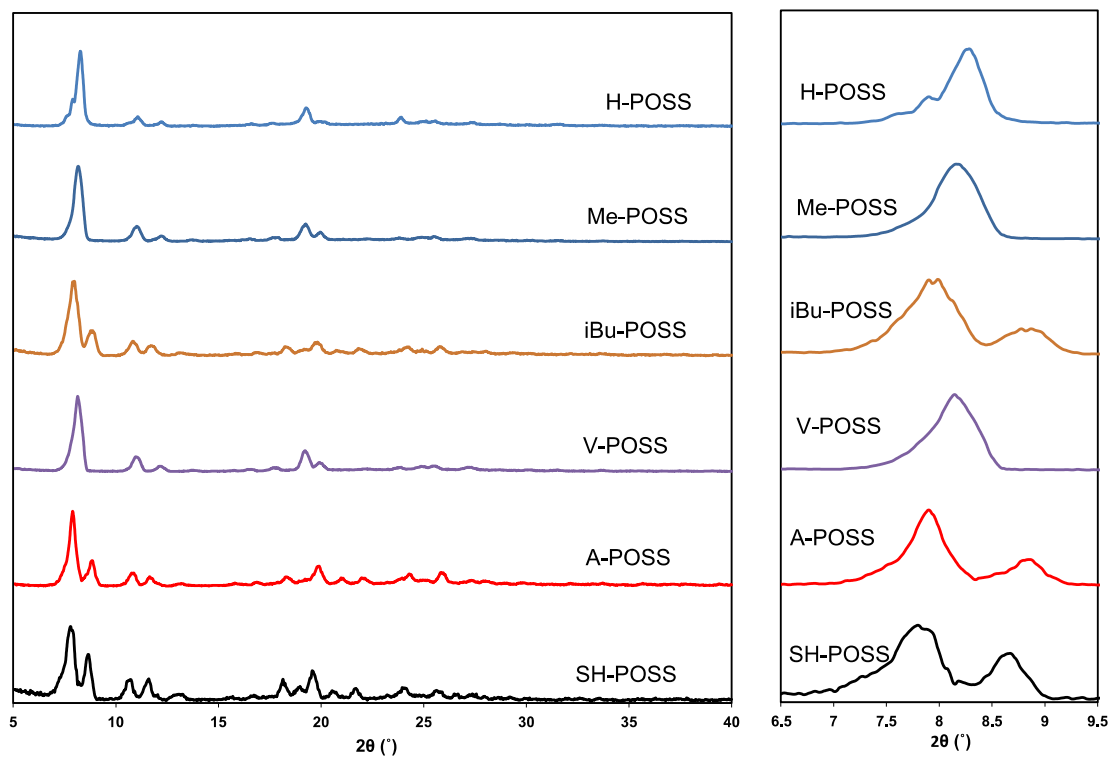


**Figure S2** XRD traces of the mono-functionalized POSS (R-POSS).

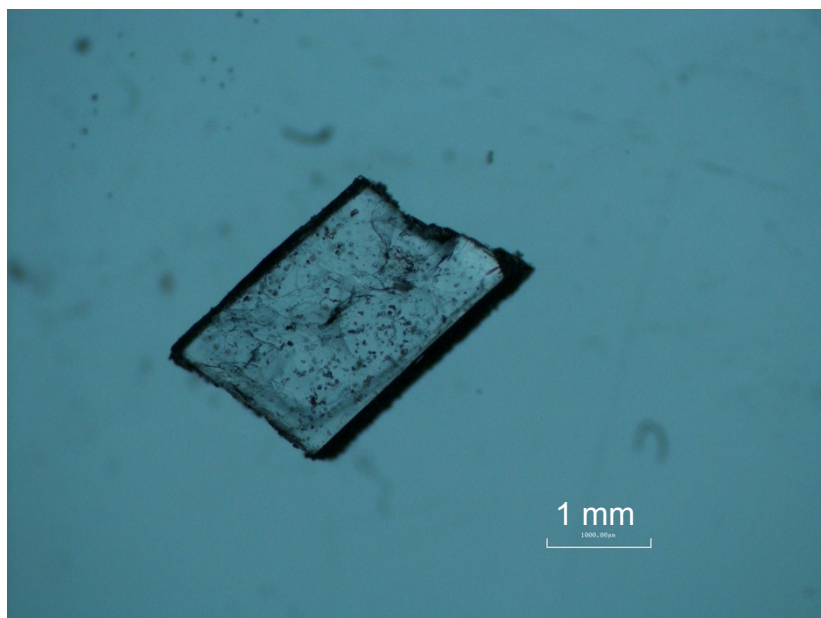


**Figure S3** Optical microscopic image of a co-crystal of A-POSS and SH-POSS (1:1).

POSS solid solutions were also obtained in the different combinations of monofunctionalized heptaioisbutyl-substituted octasilsesquoxanes (R-POSS). Same amounts of A-POSS and V-POSS were dissolved in THF and reprecipitated by adding methanol to obtain a mixing sample. The molar ratio was estimated as 0.55/0.45 by  $^1\text{H}$  NMR analysis. A DSC analysis of the co-precipitates of A-POSS and V-POSS showed a sharp endothermic peak at 29 °C which was different from the physical mixture of A-POSS and V-POSS showed two endothermic peaks at 11 °C and 48 °C, corresponding of the endothermic peaks of A-POSS and V-POSS, respectively (Figure S4). The simple physical mixture of A-POSS and SH-POSS showed two endothermic peaks at 48 °C and 38 °C, corresponding of the endothermic peaks of A-POSS and SH-POSS, respectively, even after the first heating to 150 °C, suggesting no melting after the phase transition to 150 °C.

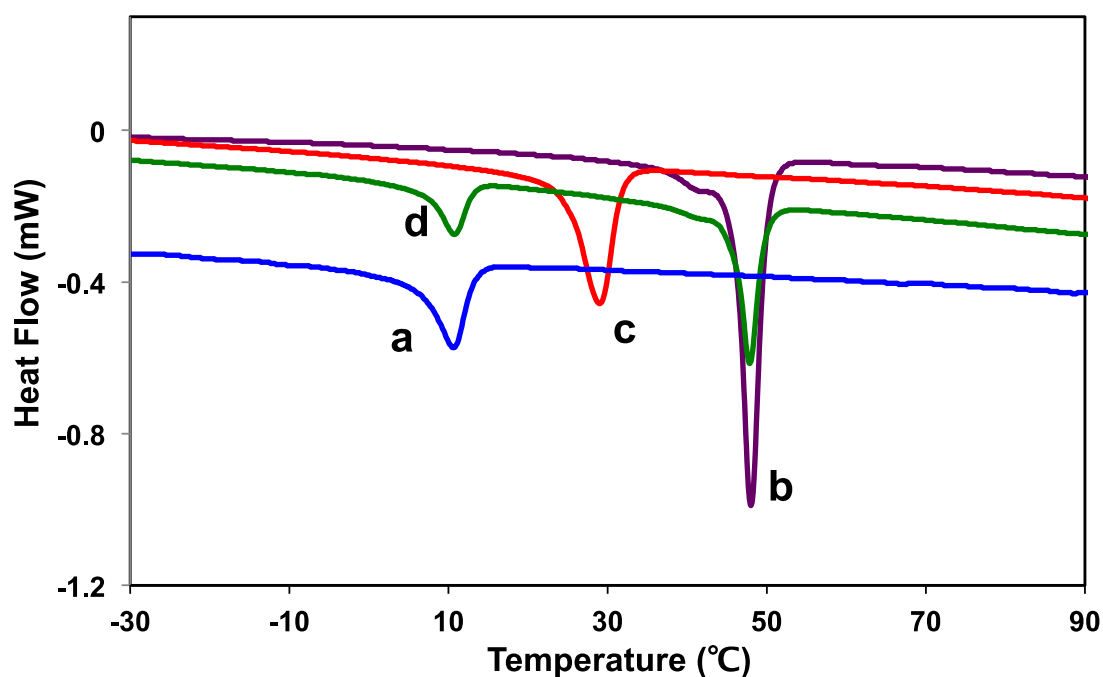


**Figure S4.** DSC data for (a) V-POSS, (b) A-POSS, (c) co-precipitates of V-POSS and A-POSS (1:1), and (d) physical mixture of V-POSS and A-POSS (1:1).